Supporting Information for

One-step sulfuration synthesis of hierarchical $NiCo_2S_4$@$NiCo_2S_4$ nanotube/nanosheet arrays on carbon cloth as advanced electrodes for high-performance flexible solid-state hybrid supercapacitors

Jinlei Xie,[a] Yefeng Yang,*[a] Geng Li,[a] Hanchun Xia,[a] Peijia Wang,[a] Peiheng Sun,[a] Xiaolong Li,[a] Haoran Cai,[a] and Jie Xiong[a]

a Department of Materials Engineering, College of Materials and Textiles, ZhejiangSci-Tech University, Hangzhou 310018, P. R. China

Email address: yangyf@zstu.edu.cn(Dr. Y. Yang)

Tel: +86-571-8684 5569

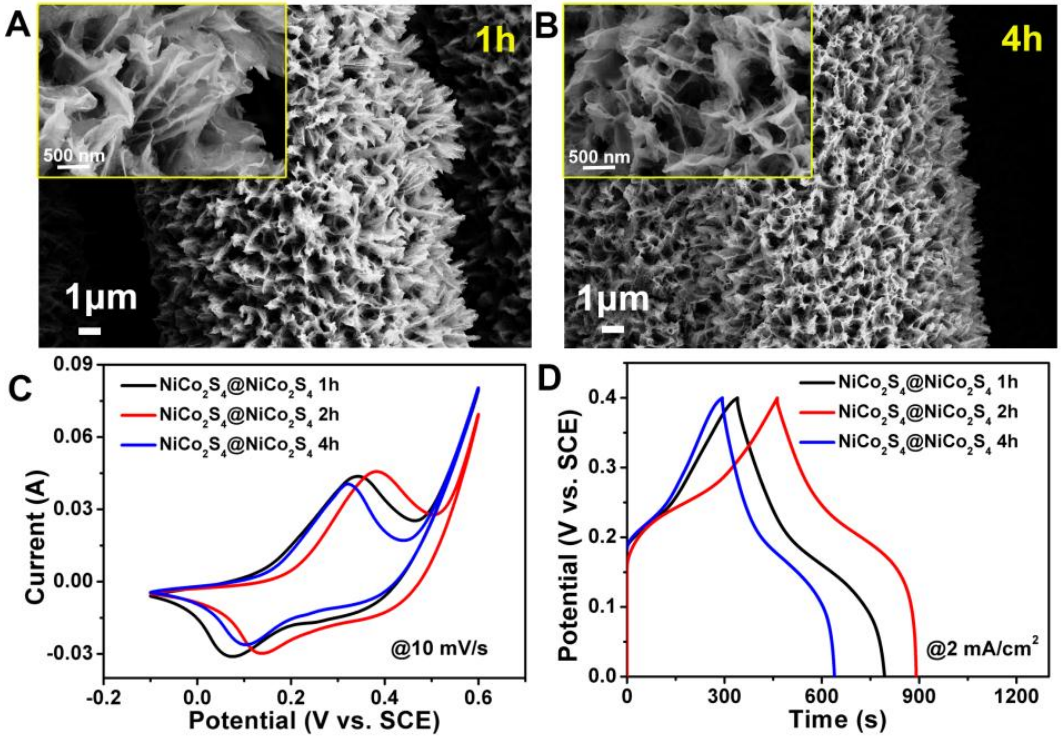

Figure S1. (A, B) SEM images of the $NiCo_2S_4$@$NiCo_2S_4$ hybrid NTSAs with different growth time of Ni-Co precursor shells: (A) 1 h and (B) 4 h; The final loading amount of $NiCo_2S_4$@$NiCo_2S_4$ hybrid NTSAs is determined to be 1.0 and 1.4 mg/cm^2, respectively. (C, D) Comparison of the electrochemical properties of the $NiCo_2S_4$@$NiCo_2S_4$ hybrid NTSAs with different growth time of Ni-Co precursor shells: (C) CV curves at a scan rate of 10 mV/s, and (D) GCD curves at a current density of 2 mA/cm^2.

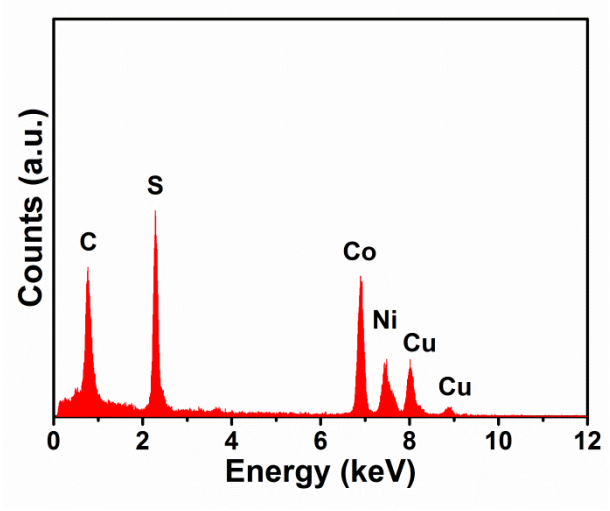

Figure S2. EDX spectrum obtained from the $NiCo_2S_4$@$NiCo_2S_4$ hybrid electrode. The Cu and C signals are from the TEM copper grids.

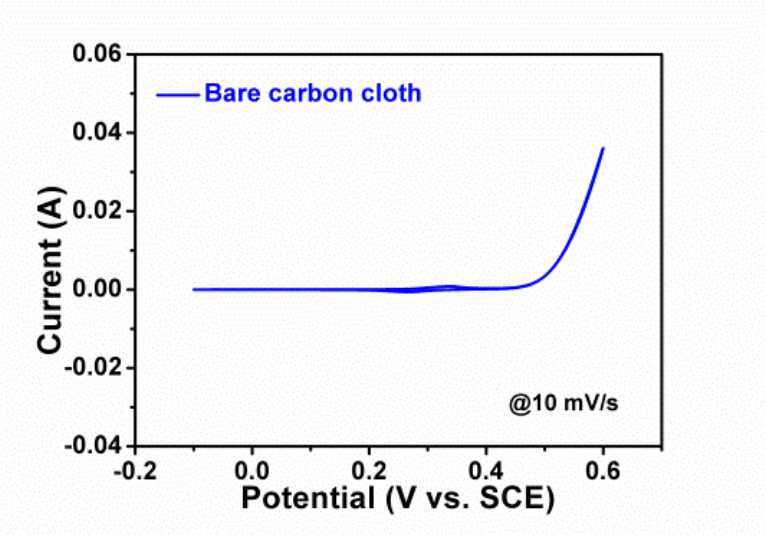

Figure S3. The CV curve of the bare carbon cloth at a scan rate of 10 mV/s**.**

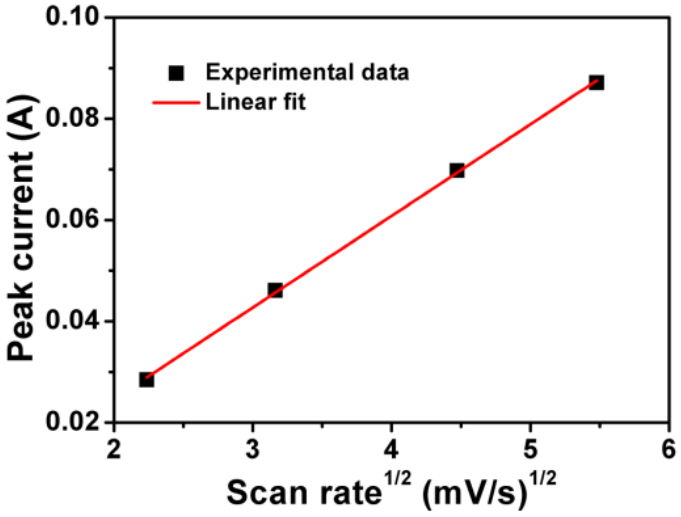

Figure S4. The linear relationship between peak current and square root of scan rate obtained from the CV curves of the $NiCo_2S_4$@$NiCo_2S_4$ hybrid electrode.

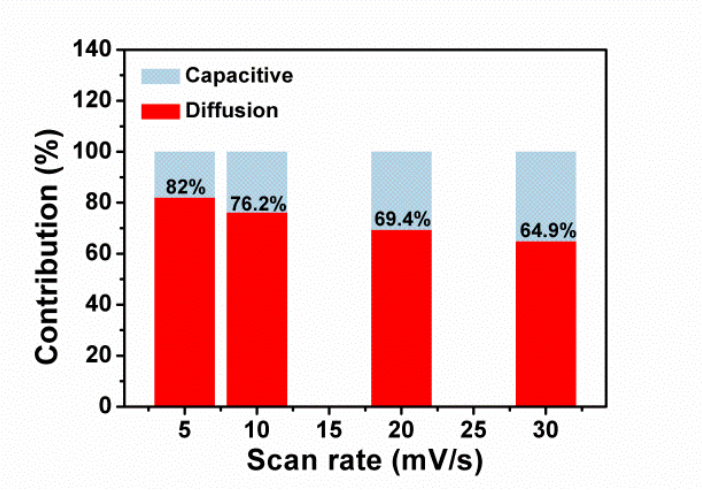

Figure S5. The contribution of capacitive and diffusion-controlled processes to the total capacity of $NiCo_2S_4$@$NiCo_2S_4$ at different scan rates of 5, 10, 20 and 30 mV/s.

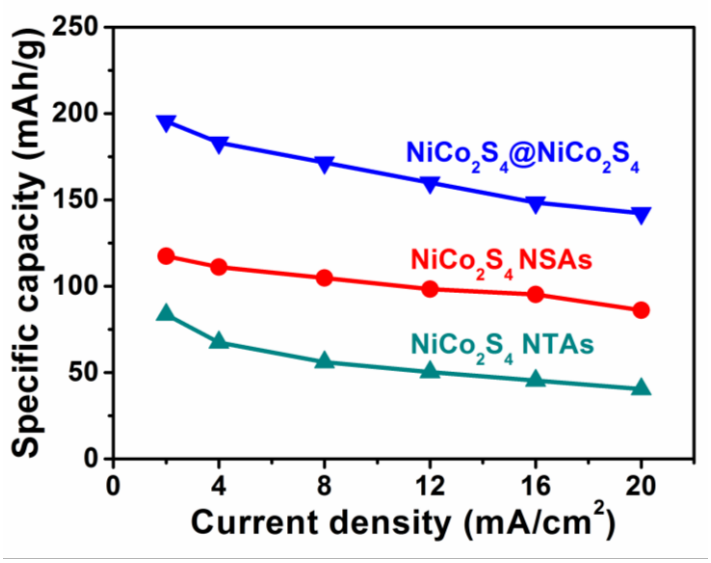

Figure S6. Varied specific capacities of the $NiCo_2S_4$@$NiCo_2S_4$ hybrid electrode as a function of current density from 2 to 20 mA/cm^2.

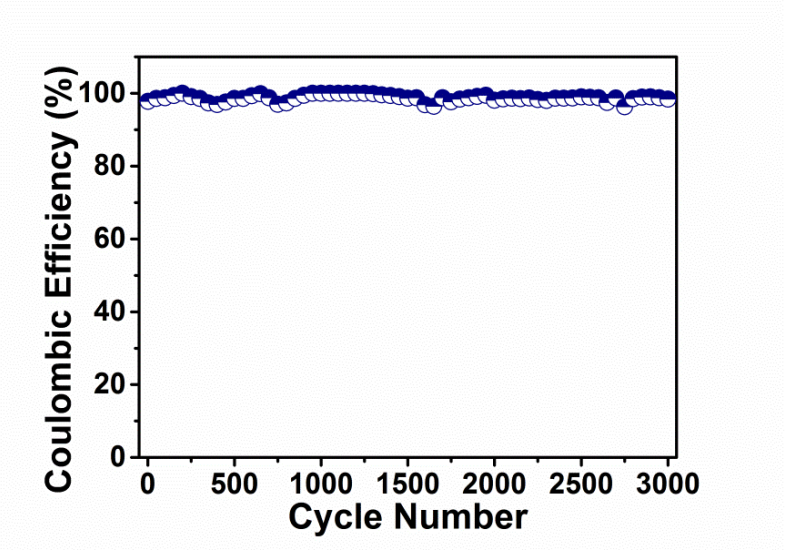

Figure S7. The variation of Coulombic efficiency for the $NiCo_2S_4$@$NiCo_2S_4$ hybrid electrode during the cycling process.

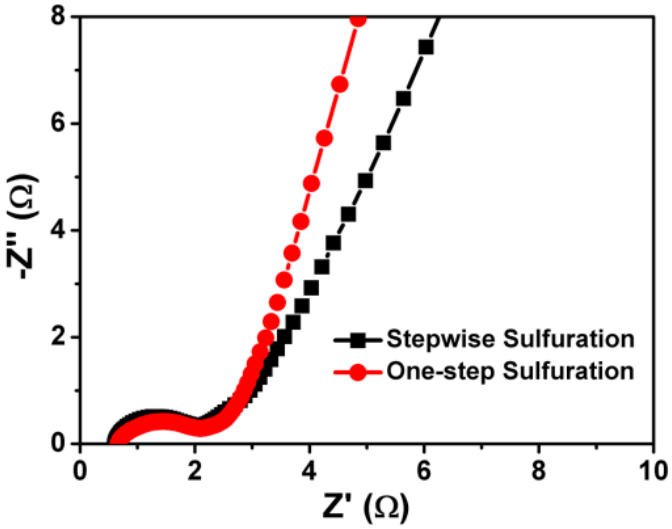

Figure S8. Comparison of the EIS spectra for the $NiCo_2S_4$@$NiCo_2S_4$hybrid NTSAs synthesized by two different pathways.

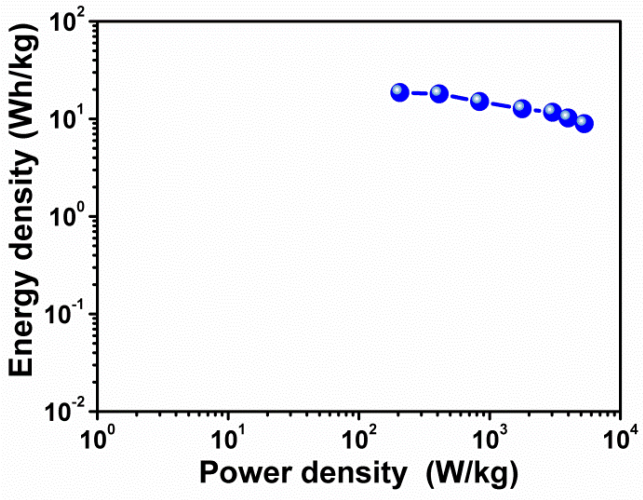

Figure S9. Ragone plot of the $NiCo_2S_4$@$NiCo_2S_4$//AC flexible solid-state HSC device, showing the relationship between the gravimetric energy density and the gravimetric power density.

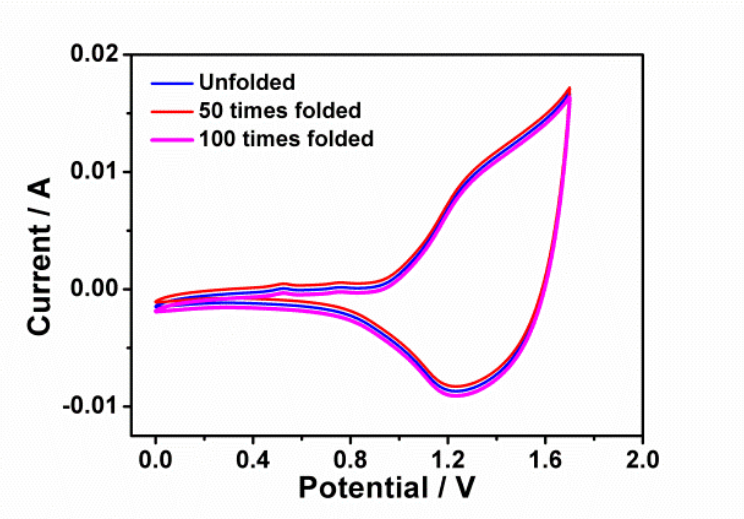

Figure S10. CV curves of the $NiCo_2S_4$@$NiCo_2S_4$//AC flexible solid-state HSC device with different folded times.